Proceedings World Geothermal Congress 2020+1
Reykjavik, Iceland, April - October 2021

Field Trial of a Surface Heat Flow Probe at the Cuitzeo Lake Geothermal Zone, Mexico

Luis C.A. Gutiérrez-Negrín, Graeme Beardsmore, Víctor H. Garduño-Monroy†, Orlando M. Espinoza-Ojeda, Salvador Almanza-Álvarez, Anson Antriasian, Shannon Egan

Geocónsul, SA de CV, CeMIE-Geo, AC, GEMex Project, Morelia, 58090, Mich., Mexico

l.g.negrin@gmail.com

Keywords: Heat Needle, Heat flow, Cuitzeo Lake, Mexico, Exploration

ABSTRACT

From September 2014 through March 2015 six 'Heat Needle' probes were deployed around the Cuitzeo Lake geothermal zone in central Mexico, to assess their functionality and outcomes in geothermal exploration. The trial was part of Project 23 of the Mexican Center for Geothermal Energy Innovation (CeMIE-Geo): "Testing probes for measuring shallow heat flow in geothermal zones". The Cuitzeo Lake is located within the Mexican Volcanic Belt and presents several geothermal manifestations in its surroundings, being the zones of Araró and San Agustín del Maíz two of the most attractive. The six Heat Needles were placed in these two zones, even though there are another two zones of interest. They proved relatively simple to deploy and retrieve. Only one Heat Needle suffered minor damage during an attempted deployment in stony ground. That Heat Needle was replaced with another, and all six were subsequently recovered in re-usable condition. Heat Needles at two sites were apparently tampered with before the end of the trial, cutting short their recording period. Also, two out of seven sensors in one Heat Needle failed to record for any of the trial period for an unknown reason. Each Heat Needle precisely recorded thermal gradient in the top 1.10 m of soil at 15-minute intervals for the duration of the trial, and made a single measurement of the thermal conductivity profile of the soil. Combining the thermal gradient records with the thermal conductivity measurements provided an estimate of surface heat flow through time at each site. Superficial heat flow values ranged from 3.5 to 17.5 W/m^2, which is up to two magnitude-orders higher than the average continental value, suggesting preliminary discharge values between 3.5 and 17.5 MW$_{th}$ per square kilometer. The conclusion is that these high values were strongly affected by the temperature of the huge shallow thermal aquifers identified in the subsoil of both areas. That is, the high values of heat flow estimated with the probes, after filtering the diurnal, seasonal and meteorological contributions, reflect the local heat discharge due to the shallow and/or sub-surface aquifers, which seem to be indicative of a deeper hydrothermal geothermal reservoir. This, in turn, tends to confirm the high geothermal potential of the Cuitzeo Lake zone, as interpreted by other geological, geophysical and geochemical surveys conducted there.

1. INTRODUCTION AND PREMISES

The Mexican Center for Geothermal Energy Innovation (CeMIE-Geo) was a project funded by the Energetic Sustainability Fund (FSE), composed in turn of 30 specific projects related to exploration, development and direct uses of geothermal energy. It officially started in 2014 and finished in April 2019, and one of those specific project was Project 23 (P23): Testing probes for measuring shallow heat flow in geothermal zones. P23 was an 18-months long project that concluded in 2016, which consisted of the deployment in some geothermal fields and areas in Mexico of 12 probes, called Heat Needles, with the purpose of assess the functionality of the probes for quantifying anomalous surface conductive heat flow for geothermal surveying. One of those areas is the Simirao-San Agustín del Maíz geothermal zone, located south of the Cuitzeo Lake, State of Michoacán, where six of the probes were placed (Fig. 1).

The Heat Needles were deployed in previously selected points of the zone and left there to automatically collect data for approximately six months, with some monitoring visits intercalated. After that period, the probes were recovered, the data processed and the results were interpreted. The Heat Needles have been designed and manufactured by the Australian company Hot Dry Rocks (HDR), but were in a prototype state when tested. The device employs sensors placed inside a pipe of stainless steel 125 cm long and 1.6 cm of external diameter. The pipe is inserted into the soil using a hand-operated electric hammer drill, powered by a portable electric generator, with sensors subsequently inserted in the pipe and left to passively monitor the shallow temperature profile at regular intervals over the trial period.

Thus, the Heat Needle is a self-contained tool for measuring conductive heat flow in the top meter of the surface. The probes combine a series of accurate and sensitive thermometers with onboard memory and a heating element for 'line source' thermal conductivity measurements, all of which were previously and precisely calibrated (for details see Beardsmore, 2012, and Beardsmore & Antriasian, 2015). The six probes of this test in Simirao-San Agustín del Maíz were placed in a vertical orientation with a maximum deviation of 2°. They contained seven onboard sensors to record temperature to ±0.0003°C precision and ±0.003°C absolute accuracy at 15-minute intervals at ground surface level, and at 10 cm, 30 cm, 50 cm, 70 cm, 90 cm and 110 cm depth. Each 96 consecutive measurements give a 24-hour average temperature for any given sensor depth, which effectively filters the large diurnal fluctuations in near-surface temperature.

At each point was obtained an in-situ thermal conductivity measurement of the ground, at the beginning and/or at the ending of the six-month trial. Each one consisted of recording the temperature response of the Heat Needle over one hour, during which it was internally heated at a constant rate of 14.9 W/m. In practice, the measurement of thermal conductivity involves calculating the gradient of a plot of temperature versus the natural log of time after heating commences once the curve reaches linearity.

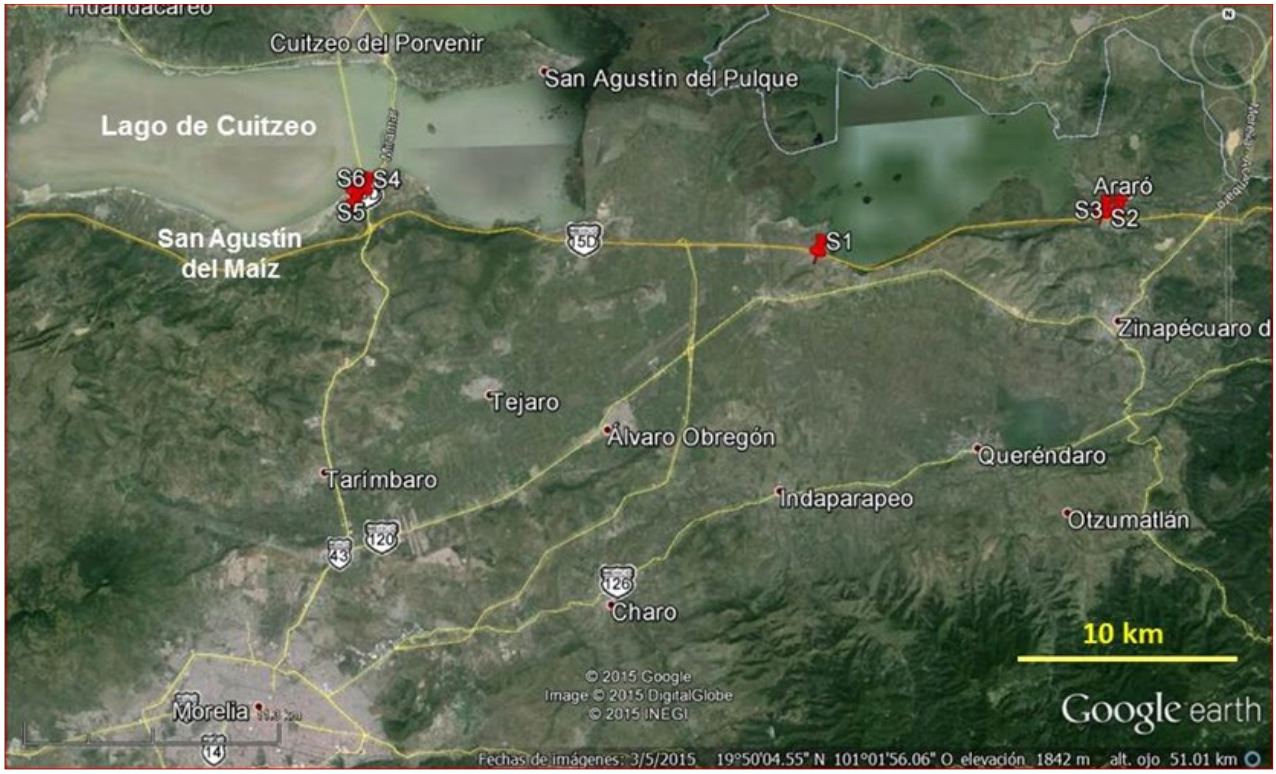

Figure. 1. Location of the six sites (S1 to S6) in Simirao and San Agustín del Maíz, Michoacán, Mexico, where the Heat Needles were tested.

The vertical conductive heat flow at any given time (Qt, W/m^2) is the product of the thermal gradient at that time (δTt / δz, K/m) and the thermal conductivity (λ, W/mK): $Q_t = \lambda \, . \, \delta T_t / \delta z$.

Where the thermal conductivity varies with depth, the heat flow can alternatively be calculated as the temperature gradient versus thermal resistance (R, m^{2}K/W), where R is the physical depth (z) divided by the average thermal conductivity between the surface and the depth (z): $Q_t = \delta T_t / \delta R$.

After the measurement period, each Heat Needle data set gives a daily average temperature profile, and the thermal conductivity profile for the point where it was placed. Applying these data to the last equation yields a daily average conductive heat flow at each site. Thus, most of heat flow variations over an extended period is then due to changes in weather systems and seasonal cycles, longer than 24 hours. As these longer period signals are similar over broad areas, observed changes in heat flow between the points can be attributed to subsurface causes, especially if they are approximately constant with time. This is the basic premise underpinning the use of Heat Needles for geothermal surveying.

2. SIMIRAO-SAN AGUSTÍN DEL MAÍZ GEOTHERMAL ZONE

Structurally, the Simirao-San Agustín del Maíz region is within the domain of the Morelia-Acambay Fault System (MAFS), characterized as a distensive system that has controlled the formation of Cuitzeo Lake and is composed of normal faults of preferential E-W and ENE-WSW strikes with dips to the north, which tilt the lithological units to the south. From a fractal analysis it is observed that the basal andesitic unit presents three fracture systems: sub-horizontal fractures (probably due to the cooling of lavas) of E-W direction, sub-vertical fractures of orientation ENE-WSW related to normal faults of the same orientation, and sub-vertical fractures of NNW-SSE direction related to normal and lateral right faults (Bermejo et al., 2016).

The Cuitzeo Basin, which includes the lake of the same name, covers almost 3400 km2, although its extension in the E-W direction has a maximum of 100 km and in the N-S direction of up to 60 km. The basin is located in the E-W Chapala-Tula system, product of the N-S distension that characterizes the Mexican Volcanic Belt (FVM) and is cut by the Tzitzio-Valle de Santiago regional strike-slip fault of NNW strike. This fault separates longitudinally two areas with different response to the distension into which the basin is divided: a graben to the east of the fault and a semi-graben to the west, with blocks tilted to the south. To the south of the lake there are thermal manifestations that can be grouped into four zones: Chucándaro in its western end, San Agustín del Maíz and San Juan Tararameo in its central portion, and Araró-Simirao in the east. Altogether, the thermal manifestations in each zone are aligned according to normal structures of approximate direction E-W (Mazzoldi et al., 2016).

In the southern region of the lake there is alkaline-neutral groundwater whose recharge zones are the mountainous limits of the valley towards the east of Zinapécuaro and the west of Morelia. In that same southern region, the direction of the underground flow is from south to north (Segovia et al., 2005), while in the southeast portion of the lake, in Queréndaro, the flow has a SE-NW direction following the local fault system (Israde-Alcántara and Garduño-Monroy, 1999).

A study by another of the CeMIE-Geo projects included a census of the thermal manifestations located at the southern part of Cuitzeo Lake and that give rise to the four mentioned geothermal zones. Thus, 32 hot springs, a cold spring and a well drilled by

the National Water Commission for the water supply for the community of Simirao were identified. In addition, from previous hydrological studies, it has been determined that in the Cuitzeo Basin there are at least two aquifers housed in fractured rocks, a deep one formed by andesitic rocks and an intermediate aquifer in rhyolitic tuffs. There is also a third sub-surface aquifer, hosted in fluvial-lacustrine sediments whose phreatic level crops out in the Cuitzeo Lake. These fluvial-lacustrine sediments seem to act as a kind of seal-cap of the thermal reservoir that feeds the springs (Rentería and Garduño, 2016).

Through a geomagnetic survey and recent geological-structural studies, a conceptual geological model has been constructed that explains the presence of hydrothermal manifestations in the zones located in the south-central part of the present-day Cuitzeo Lake near the villages of San Agustín del Maíz and San Juan Tararameo. According to this model, one or more N-S oriented faults, originated as part of the Basin and Range system, allowed the ascent of a magmatic body whose surface evidence is a small volcanic island in the center of the lake. The body would have been trapped under the lacustrine clay sediments probably during the Late Pleistocene, and thus would be the heat source of the probable geothermal system, whose fluids come from deep regional aquifers heated by the intrusive body and mixed with their own fluids. The geothermal fluids ascend to the surface in certain points, through the faults of the other system, of approximate direction E-W, which are low angle faults with deep listric features, and belong to the MAFS. These faults are more active today (Mazzoldi et al., 2016).

On the other hand, in the geothermal zone of Araró-Simirao the main area of thermal manifestations is located about 4 km north of the city of Zinapécuaro. The Federal Commission for Electricity (CFE) has carried out at least a couple of exploration campaigns in the area, including the drilling of an exploratory well in the early 1990s, called Z-3, which reached a depth of 1344 meters and it flowed intermittently producing hot water. The maximum temperature recorded in the well was 135°C at 550 meters depth, which dropped to 111°C at the bottom of the well. In this zone the most relevant local structures are the Huingo and Araró-Simirao faults, both normal and general direction E-W, through which most of the hot springs are flowing. These springs present some gases and superficial temperatures ranging from 30°C to the water boiling point (Viggiano-Guerra and Gutiérrez-Negrín, 2003).

In particular, the manifestations of San Nicolás Simirao have temperatures between 39 and 93°C spreading in an area of about 10 hectares, with water of sodium-chloride type and average salinity of 2340 mg/liter. It has been considered that in the underground of this area there may be a geothermal hydrothermal system with temperatures between 220 and 250°C at a depth greater than that reached by well Z-3 (Viggiano Guerra and Gutiérrez-Negrín, 2003). Just inside this area is located the mentioned exploratory well Z-3, but also there were placed two of the Heat Needles tested in this project, which were located at sites S2 and S3, as described below.

3. LOCATION OF THE PROBES

The six Heat Needles in this area were placed between September 22 and 23, 2014 in six different sites, which are indicated in Figure 1.The sites were chosen based on accessibility, security and proximity to known or suspected geothermal features. The probes were left in their sites taking a series of records every 15 minutes during an approximate period of six months, during which three supervision visits were made, in the months of October and December 2014 and February 2015.

The objective was to collect two sets of data at each site: i) A passive record of ground temperature to sub-millikelvin precision and ±0.003 K absolute accuracy at the air–soil interface and at 10 cm, 30 cm, 50 cm, 70 cm, 90 cm and 110 cm depth at 15-minute intervals for the duration of the trial. These data provided precise records of changes in shallow thermal gradient over time; and ii) The temperature response of the Heat Needle to an active injection of heat over a one-hour period. These data provide information about the thermal conductivity structure of the ground. Conductive heat flow is the product of thermal gradient and thermal conductivity.

The probes were recovered at the end of March 2015, and the measurements were downloaded into Excel files. These files, together with those that contained the data of the thermal conductivity measurements, were processed by the company HDR at its facilities in Melbourne, Australia. The most relevant technical information of each of the six sites in this area is summarized below.

It's important to keep in mind that the field trial was not intended as an exploration or mapping exercise, but rather a test of the functionality of the Heat Needles under field conditions. Shallow temperature surveys have previously demonstrated that a maximum spacing of two to three hundred meters would be best to image heat flow variation across active geothermal systems (Coolbaugh et al., 2014).

Site S1. Queréndaro Station. This site was located practically between the zone of Simirao and that of San Agustín del Maíz, on the periphery of the town Estación Queréndaro, relatively close to some hot springs. Its UTM coordinates are 295,106E, 2,199,977N, elevation 1865 masl. Dates of placement and extraction: September 22, 2014 and March 22, 2015. Effective period of temperature data registration: September 23, 2014 to February 10, 2015.

Site S2. Simirao hybrid project. It is located in the area of Simirao, about 12.6 km east of site S1 (Fig. 1), on privately owned land where the exploratory geothermal well Z-3, drilled by the CFE, is located. Its UTM coordinates are 307,849E, 2,201,310N, elevation 1912 masl. Dates of placement and extraction: September 22, 2014 and March 22, 2015. Effective period of temperature data registration: September 23, 2014 to March 22, 2015.

Site S3. La Salud Spa. It is a site very close to the S2, located about 600 meters to the east, inside a small privately owned spa located on the outskirts of the town of San Nicolás Simirao and very close to natural hot springs. Its UTM coordinates are 308,481E, 2,201,328N, elevation 1895 meters above sea level. Dates of placement and extraction: September 22, 2014 and March 22, 2015. Effective period of temperature data registration: September 23, 2014 to March 22, 2015.

Site S4. Los Manantiales Spa. This site is part of the geothermal zone of San Agustín del Maíz, and is located about 20 km west of site S1 (see Figure 1). It is also inside a spa and recreational center of private property, called Los Manantiales. Near the spa there is a well that supplies hot water for swimming pools and baths. Its UTM coordinates are 274,786E, 2,202,853N, elevation 1860 masl.

Dates of placement and extraction: September 22, 2014 and March 23, 2015. Effective period of temperature data registration: September 25, 2014 to March 23, 2015.

Site S5. Los Estanques Spa. The site is in a small resort on the outskirts of San Agustín del Maíz and about 500 meters west of site S4. Near the resort is a hot spring that feeds the pools. Its UTM coordinates are 274.276E, 2,202,680N, elevation 1815 meters above sea level. Dates of placement and extraction: September 22, 2014 and March 23, 2015. Effective period of temperature data registration: September 25, 2014 to March 23, 2015.

Site S6. La Ciénaga Restaurant. This site is located about 500 meters south of site S5 (see Figure 2). It is also on the outskirts of San Agustín del Maíz, next to a tourist restaurant called La Ciénaga, near a group of hot springs. Its UTM coordinates are 274,339E, 2,202,228N, elevation 1886 masl. Dates of placement and extraction: September 23, 2014 and March 23, 2015. Effective period of temperature data registration: September 25, 2014 to January 24, 2015.

4. PROCESSING RESULTS

Following are presented in certain detail the case of the site S1, as an example of the type of activities done for every site, and then are presented the results for all the Heat Needles.

A reliable temperature record was collected from initiation to 10 February 2015 in the site S1. Time stamps were recorded every 15 minutes until the Heat Needle was deactivated and extracted on 22 March 2015. The internal clock on the Heat Needle recorded the time of the final temperature datum as 16:21 on 22 March 2015; 33 minutes and 16 seconds ahead of the true time of 15:47:44. This suggests that the internal clock ran an average of ~11.0 s per day fast over the 180-day trial.

Standard processing of the raw temperature data included the following steps:

- Conversion of digital records to temperatures
- Correction of recorded times for drift in internal clock
- Re-sampling of records to precise quarter-hour times by interpolation
- Cropping of record to fully overlap with other records in the same survey

Figure 2 shows the full record of temperatures for the first 30 days of the trial, and Figure 3 the daily average of recorded temperatures (centered on midnight UTC time each day) for the entire trial period. The full record shows that surface temperature varied on a daily cycle with a peak-to-trough amplitude averaging ~15°C. The 24-hour average effectively filtered the daily volatility and revealed weekly fluctuations in mean surface temperature with peak-to-trough amplitude on the order of 2-3°C. These are likely related to the passing of weather systems over the trial area. The annual temperature cycle is also evident in the trend of decreasing then increasing surface temperature over the course of the six-month trial. Note that in this case (S1) the temperature sensors stopped recording on 10 February 2015 (see Fig. 3), probably due to some tampering from locals.

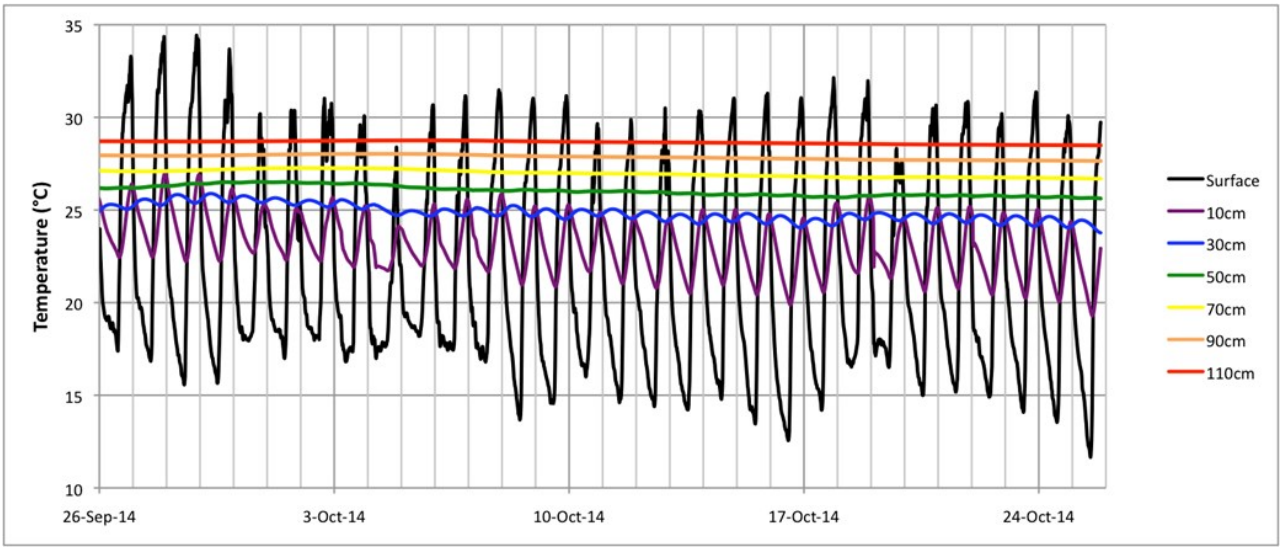

Fig. 2. Detail of temperature record for first month at site S1.

The full and filtered temperature records capture the diffusion of surface temperature fluctuations into the ground, overprinting a general increase in temperature with depth. As predicted by the diffusion equation, progressively deeper sensors show an increasing time lag and a decay in amplitude of the recorded surface temperature signal, both of which are a function of the thermal diffusivity of the ground.

A successful thermal conductivity measurement was carried out over the time interval (UTC time) 14:58-15:58 on 23 September 2014, just prior to initializing temperature logging. Temperature records at 10 cm and 30 cm depth were corrected for the mean drift in sub-surface temperature observed over the same time interval on the subsequent four days. Assuming that the Heat Needle

approximated an 'infinite line source' of heat at a rate of 14.90 ± 0.04 W/m, the resulting log-linear temperature increases observed at sensor depths (Figure 4) imply thermal conductivities of:

10 cm: 0.805 ± 0.003 W/mK

30 cm: 0.772 ± 0.003 W/mK

50 cm: 0.943 ± 0.003 W/mK

70 cm: 0.843 ± 0.003 W/mK

90 cm: 1.019 ± 0.003 W/mK

110 cm 1.4 ± 0.2 W/mK

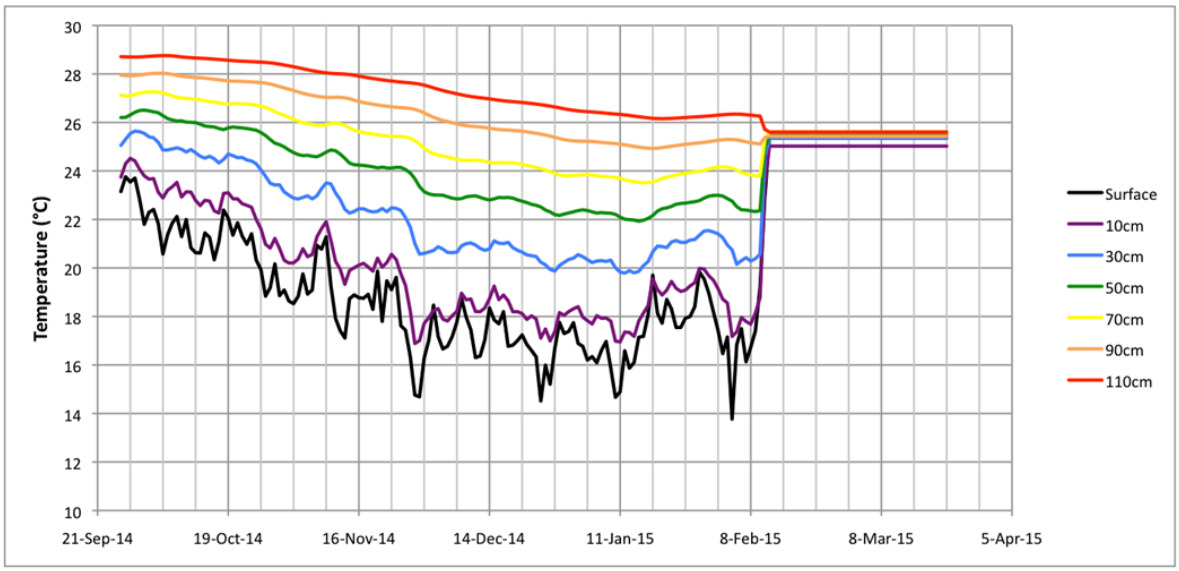

Fig. 3. Daily 24-hr average temperature centered on midnight (UTC time) for full record length at site S1.

The sensor at 110 cm lies near the deepest extremity of the internal heating element so does not meet the 'infinite line source' approximation. That sensor does not yield a reliable conductivity estimate by the same method as the others. The value for 110 cm was inferred from the observed temperature at that depth and the Bullard plots presented below.

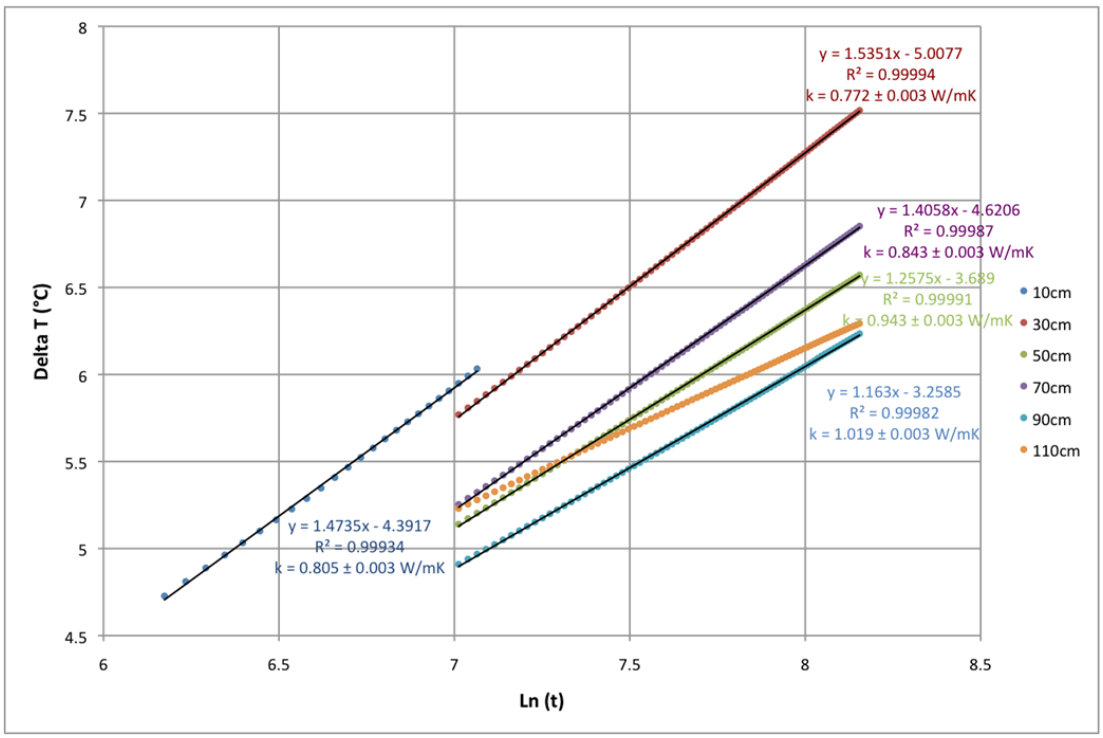

Fig. 4. Temperature increase versus the natural log of heating time for site S1.

In a steady state conductive setting, temperature increases linearly with thermal resistance at a gradient equal to the conductive heat flow. Thermal resistance is the integral of physical depth divided by thermal conductivity. The thermal resistance from the surface to each sensor depth was estimated from the thermal conductivity values above. Then the mean conductive surface heat flow was calculated for each day from the gradient of the best-fit linear regression of the 24-hour mean temperature versus thermal resistance. A 'Bullard plot' (temperature versus thermal resistance) varies from linear if conductive heat flow is not steady state, or if there is a component of advective heat flow. Close to the surface, heat flow is not steady state; the periodic heating by the sun affects it. A straight line of best fit, however, provides an estimate of the mean conductive heat flow at any given moment. Figure 5 shows a sample of Bullard plots at one-month intervals during the recording period at S1. Each plot is labeled with its gradient (Q = heat flow) and the Pearson product moment correlation coefficient 'r^2' values indicating degree of linearity.

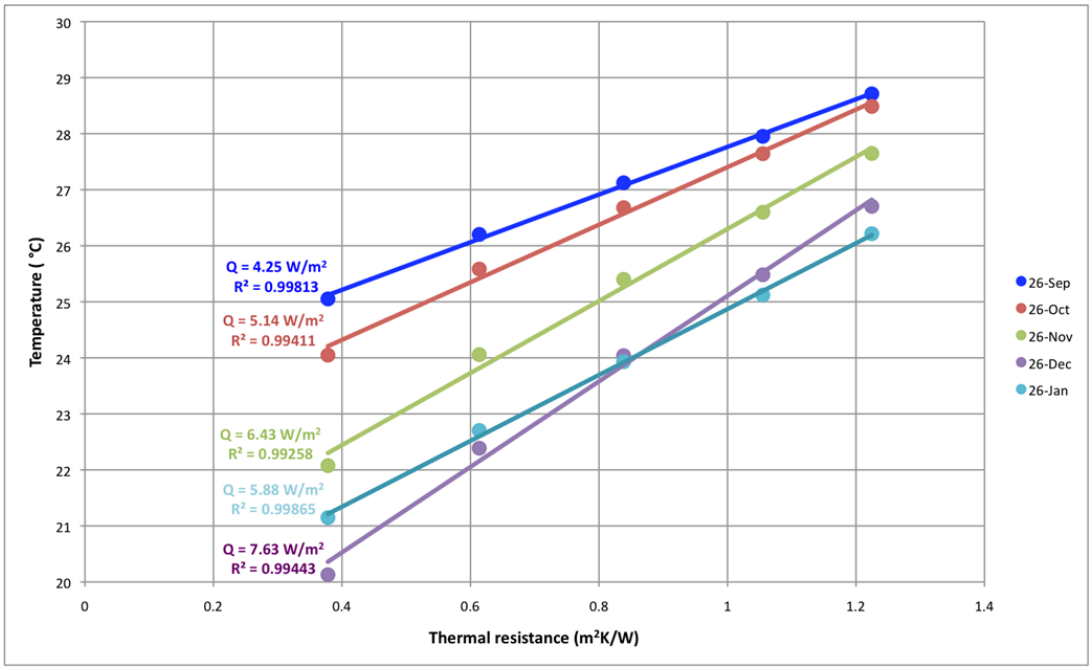

Fig. 5. 24-hr average temperature versus thermal resistance (Bullard plot) for site S1.

Variation in conductive heat flow through time is inferred from the variation in gradient of the Bullard plot at successive time steps. The bold red line on Figure 6 presents the inferred conductive surface heat flow as a function of time. The rise in inferred heat flow over the first three months of the record is likely a result of the seasonal drop in surface temperature over that period. A seasonal correction can be approximated from the observed surface temperature drift between the equinox and the solstice (~6.5°C), the thermal diffusivity of the ground estimated from the diffusion of the daily temperature signal to 110 cm (2.6×10^{-7} m^2s^{-1}), and an assumption of a 365-day periodic surface temperature cycle. The brown line on Figure 6 shows the 'corrected' heat flow. Temperature records ceased on 10 February 2015 due to physical damage to the equipment caused by apparent tampering by persons unknown. The logger continued to record null values at regular 15-minute intervals because connection to the sensors was severed.

The best estimate of geothermal heat flow at this location is ~3.5 W/m^2 from the 'corrected' curve on Figure 6. This value remains relatively constant over the measurement period. The intervals of relatively elevated inferred heat flow (~4.5 W/m^2) from late November to mid-January and early February can be traced on Figure 3 to sustained decreases of 2–3°C in surface temperature relative to the earlier trend. The same goes for heat flow variations with periods on the order of one to two weeks. Note that 3.5 W/m^2 is about 50 times the mean global continental heat flow (Beardsmore and Cull, 2001), which indicates a shallow and/or active heat source beneath this site.

Data and results from the other five sites, including S1, are presented in Table 1.

Table 1. Heat flow calculated with Heat Needles in the six sites of the Simirao-Araró zone.

Site	Location	Area	Heat Flow (W/m^2)	Remarks
S1	Queréndaro Station	Intermediate	3.5	Data up to 10 Feb 2015
S2	Simirao Hybrid Plant	Simirao	7.5	
S3	La Salud Spa	Simirao	17.5	Two thermal conductivity tests
S4	Los Manantiales Spa	San Agustín del Maíz	4.0	
S5	Los Estanques Spa	San Agustín del Maíz	6.0	Two sensors failed
S6	La Ciénaga Restaurant	San Agustín del Maíz	12.5	Data up to 24 Jan 2015

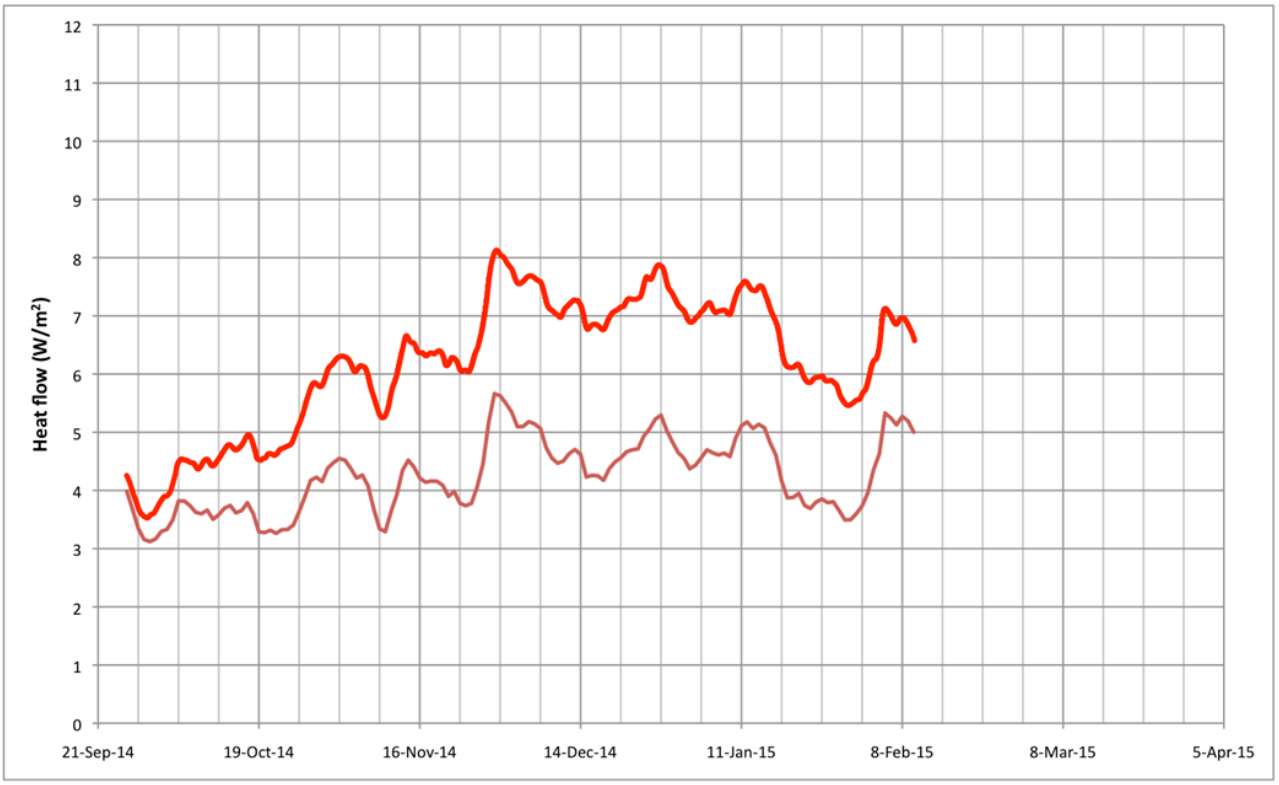

Figure. 6. Inferred conductive surface heat flow versus time for site s1 (bold red); approximately corrected for seasonal surface temperature (brown). Temperature records ceased on 10 February 2015 at this site.

5. PERFORMANCE OF THE HEAT NEEDLES

Once prepared and calibrated in the laboratory, placing the Heat Needles in the field is quick and easy. The process includes pre-drilling the hole, placing the stainless steel pipe, introducing the Heat Needle sensors and logger, and initializing it to start taking readings. The technical procedure for initializing the recorder is relatively simple.

The procedure for measuring the thermal conductivity at each site is also relatively simple and fast. However, in this project some problems and delays were experienced with the energy source used to transmit electric current to the Heat Needle and generate the heat to be injected into the ground, to then measure the conductivity of the same. The original untested prototype design of the company HDR, which was a plastic box with a serial arrangement of sixteen alkaline commercial batteries type D, 1.5 volts, did not work due to the overheating of the boxes, which later was understood to be due to the internal resistance of the alkaline batteries themselves. The option finally used was a set of two motorcycle batteries of lead acid, connected in series, each of 12 volts and more than 9 amperes-hour. It was sufficient to run all tests in all places on a single charge.

On the other hand, the operation of the Heat Needles during its automatic operation, taking records every 15 minutes along an average of six months, was satisfactory. In the areas of Simirao-San Agustín del Maíz, a single fail not attributable to external causes was detected, which was the case of probe at site S5, where a pair of sensors failed, although it was still possible to estimate the heat flow from the surviving five sensors.

The final recovery of the probe and the extraction of the pipe that contains it was equally rapid. Once the accumulated records have been downloaded for the six months (or less) of automatic operation, it is advisable to run a thermal conductivity test, even if it was previously obtained during the placement of the Heat Needle. After that, the Heat Needle is recovered and the pipe containing it is unearthed, for which the use of a portable mechanical jack is sufficient.

In summary, it can be concluded that the prototype Heat Needle tested in this geothermal zone works with sufficient reliability.

With regard to the processing of temperature and thermal conductivity data, this was carried out using an algorithm that only allowed an accuracy of ± 0.5 W/m^2, which is quite greater than the accuracy of ± 0.01 W/m^2 for which the Heat Needles are designed. This lower accuracy is not due to the quality of the data collected in the field, but to the early stage of algorithm development.

6. CONCLUSIONS

Figure 7 shows the mean daily surface temperatures recorded at all six sites presented on the same axes. While there is clearly a strong correlation between the sites, there are also some significant differences, with scatter as great as 3°C on any given day. If the surface temperatures were perfectly correlated, then differences in observed shallow heat flow would be due entirely to subsurface effects (geothermal heat and thermal diffusivity). The variations in surface temperature add an extra level of complexity to the processing and interpretation of the results. Specifically, the different sites required different assumptions of surface temperature variation in the application of the seasonal drift correction.

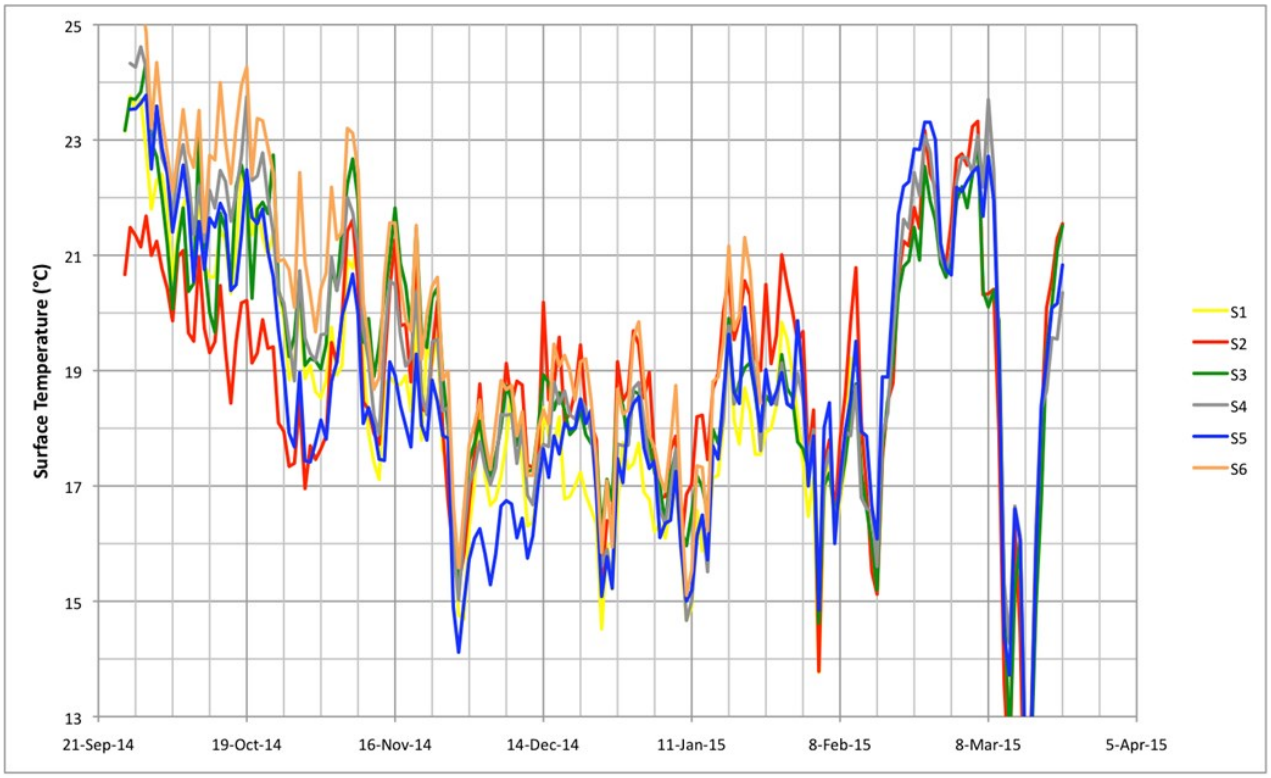

Fig. 7. 24-hr mean surface temperature records for sites S1 to S6.

Figure 8 shows the interpreted conductive surface heat flow through time at the six sites on the same set of axes. Figure 9 presents the surface heat flow with approximate seasonal corrections. There is a strong correlation in the short period (one to two weeks) features across sites, which are due to surface weather events. The relative differences in heat flow between sites are also apparent on both figures (with the possible exception of the difference between sites S2 and S5, which is more apparent on Figure 9). In fact, the relative heat flow between sites was largely determined in the first week or two of the trial, but that is possibly because the beginning of the trial coincided with the equinox (the time at which the seasonal variability in heat flow is theoretically at a minimum).

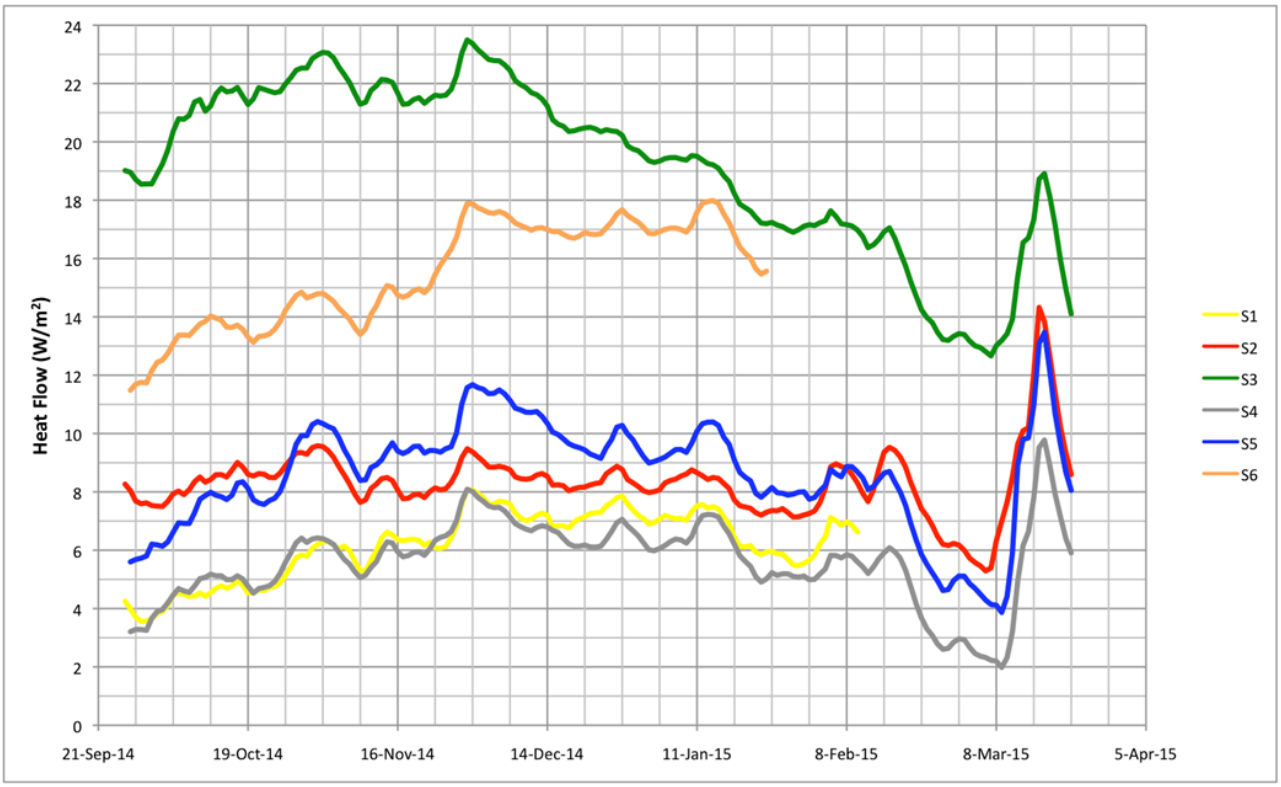

Fig. 8. Interpreted heat flow records for sites S1 to S6.

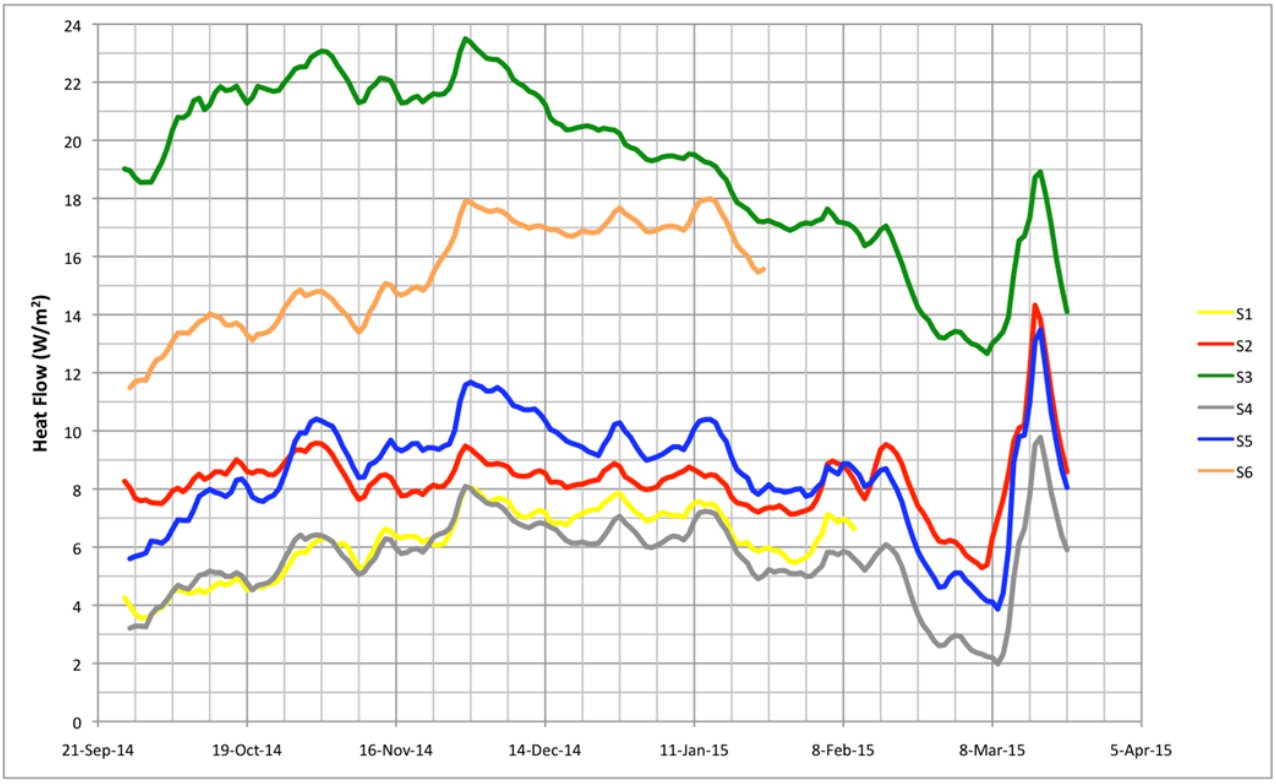

Fig. 9. Interpreted heat flow records with approximate seasonal corrections for sites S1 to S6.

The approximate seasonal corrections applied to all the data only took into account the annual temperature cycle and coarse estimates of thermal diffusivity. A more sophisticated correction should take into account all the signal frequencies, especially the 'weather systems' cycles that usually have shorter cycles of the order of two to four weeks, and more robust diffusivity determinations. It is possible to create algorithms that include such corrections in an integral data processing system. Beardsmore (2020) reports on algorithm developments subsequent to this trial that have improved resolution to ± 0.05 W/m^2.

Regarding the heat flow results, in all the sites an extremely high heat flow was obtained, as shown in Table 1, which is much higher than the average measured in the continents: the lowest heat flow value at site S1 is almost 54 times higher than the average value, while the maximum value at site S3 is almost 270 times higher, that is, two orders of magnitude greater.

These high values estimated with the Heat Needles were strongly affected by the temperature of the shallow thermal aquifers. That is, the high values of heat flow estimated with the probes, reflect the local heat discharge due to the shallow and/or sub-surface aquifers.

Evidently, the shallow and sub-surface thermal aquifers identified in Simirao and San Agustín del Maíz appear to be an expression of a deep geothermal reservoir. In fact, a preliminary interpretation, based on the geothermal characteristics of both zones that have been previously described and complemented with these values of heat flow, is that a probable deep geothermal reservoir is located in some point close to site S1, with two discharges or up-flows to the east (sites S2 and particularly S3) and to the west (sites S4, S5 and especially S6). Or, alternatively, it could be two small individual deep geothermal reservoir, with almost vertical discharges.

To assess these or other interpretations in more detail, more data are obviously needed. A systematic measurement of the surface heat flow in those areas, or in others, as part of an exploration campaign in a new field, would have to consider the use of several probes arranged in a grid or going through structures that are considered of interest, with a general spacing of ~300 m.

DEDICATION

Authors want to dedicate this paper to the memory of our coauthor Víctor Hugo Garduño-Monroy who passed away on October 15, 2019, in Mexico City. AERIPA.

REFERENCES

Beardsmore, G.R.: Towards a shallow heat flow probe for mapping thermal anomalies. Proceedings 37th Workshop on Geothermal Reservoir Engineering, Stanford University, Stanford, CA, January 30 - February 1 (2012).

Beardsmore, G.R.: A surface conductive heat flux tool to delineate geothermal reservoirs. Proceedings World Geothermal Congress, Reykjavik, Iceland, 27 April – 1 May (2020).

Beardsmore, G., and J.P. Cull: Crustal Heat Flow: A Guide to Measurement and Modelling. Cambridge University Press, Cambridge, UK, 321 p. (2001).

Beardsmore, G.R., and Antriasian, A.: Developing the 'Heat Needle'—a tool for cost effective heat flow mapping. Proceedings World Geothermal Congress, Melbourne, Australia, 19–25 April (2015).

Bermejo Santoyo, G., Jiménez Haro, A., Nájera Blas, S.M., Vásquez Serrano, A., and Garduño Monroy, V.H: Evaluación de los controles estructurales del fracturamiento como base para la creación de un modelo de fracturas discreto (MFD) del yacimiento geotérmico de San Agustín del Maíz, Mich. Proceedings of the XXIII Annual Congress of Asociación Geotérmica Mexicana, Morelia, Mich., 10-11 March (2016) (In Spanish).

Coolbaugh, M., Sladek, C., Zehner, R., and Kratt, C.: Shallow temperature surveys for geothermal exploration in the Great Basin, USA, and estimation of shallow aquifer heat loss. GRC Transactions, 38, 115-122 (2014).

Israde-Alcántara, I., and Garduño-Monroy, V.H.: Lacustrine record in a volcanic intra-arc setting: the evolution of the Late Neogene Cuitzeo basin system (central-western Mexico, Michoacán). Palaeogeography, Palaeoclimatology, Palaeoecology, 151(1), 209-227 (1999).

Mazzoldi, A., Guevara-Alday, J.A., Gómez-Cortés, J.J., and Garduño-Monroy, V.H.: Papel de estructuras Basin and Range en la formación del sistema geotérmico al centro-sur del Lago de Cuitzeo, segmento central del Cinturón Volcánico Mexicano. Proceedings of the XXIII Annual Congress of Asociación Geotérmica Mexicana, Morelia, Mich., 10-11 March (2016) (In Spanish).

Rentería Ortega, A.V., and Garduño Monroy, V.H.: Estudio hidrológico del Graben de Cuitzeo, Mich., enfocado a la caracterización geoquímica e isotópica de los acuíferos y su relación con el yacimiento geotérmico. Proceedings of the XXIII Annual Congress of Asociación Geotérmica Mexicana, Morelia, Mich., 10-11 March (2016) (In Spanish).

Viggiano Guerra, J.C., and Gutiérrez Negrín, L.C.A.: Régimen de flujo hidrotermal en la zona geotérmica de Araró, Michoacán. Ingeniería Hidráulica en México, Vol. XVIII, No. 1, (2003), pp. 39-53 (In Spanish).